Original Article

ACLSDN: A Heuristic Face Recognition Framework with Adaptive Cascaded Deep Learning using Spectral Feature Selection

Santhosh Shivaprakash[1], Sannangi Viswaradhya Rajashekararadhya[2]

[1,2]Department of Electronics and Communication Engineering, Kalpataru Institute of Technology, Tiptur, Tumkur District, Karnataka, India

[1]Corresponding Author : santhukit@gmail.com

Abstract - In recent times, most of the Facial Recognition framework has shown better outcomes in a constrained environment. Due to its high usage, the FR has gained increased attention in the research field. However, it has faced various issues in the real-time application, such as facial disguise designing in facial features, temporal variations, and low-quality images. Therefore, there is a requirement for significant techniques for detecting and identifying the human face. This paper has implemented an effective FR technique. The adequate dataset relevant to the FR process is initially gathered from the standard dataset. Then, the images are pre-processed with the aid of the median filtering process to obtain the pre-processed images. Then, it is given to the three level-Discrete Wavelet Transform (DWT), which is used to attain the spectral features. Then, the features from the spectral features are optimally chosen by using the Improved Horse Herd Optimization algorithm termed (IHHO) derived from Horse Herd Optimization (HHO). Further, it is subjected to the Adaptive Cascaded framework termed ACLSDN, designed using Long Short Term Memory (LSTM) and Deep Neural Network (DNN) model. It is carried out by averaging the score attained from both the LSTM and DNN models for attaining the classified outcomes in maximized accuracy. Here, the same IHHO algorithm is used for optimizing the parameters in the LSTM and DNN frameworks. Finally, the effectiveness of the designed FR model is validated using various metrics and shows maximized accuracy value.

Keywords - Adaptive Cascaded Long Short Term Memory, Deep Neural Network, Face Recognition, Improved Horse Herd Optimization, Three Level-Discrete Wavelet Transform.

1. Introduction

In recent times, FR has been considered a crucial process in computer vision. Even though it is not at all a new concept but the outbreak in electronic appliances has been realized, which has resolved various issues [34]. It has been widely utilized, particularly in the field, with strict measures such as banks, airports, police stations, and so on [10]. The FR framework has been usually presented along with the facial features that include mouth, nose, and eyes, which are non-occluded faces [11]. It has become an essential part of the study of machine learning, pattern recognition, and machine vision [12,21]. Concerning the FR model, the system has initially selected a face, which is more likely to be that of the desired face-to-training face, and then it has been determined as the final outcome. The term FR is implemented in the 1960s [13]. In the initial stage, the inventors generated a semi-automatic FR framework. Some of the FR[14] application involves access control, detection of the person in international centers of transition, security applications in the banks, forensic and medical apps, monitoring, and various

fields [35]. Moreover, the human face has acquired a huge amount of details, which has been utilized in various models like tracking of security cameras, audience recording, electronic consumer experience management, Human-Computer Interaction (HCI), description of gender and gestures, forecasting images and restoration apps, facial identification as well as artificial age classification [15].

Generally, the FR model has compressed of four different stages detection, facial feature extraction or classification, representation, and alignment [16]. In considering the FR framework, the crucial issues are the feature depiction system that is used to retrieve the features along with the best method for an acquired biometric trait to be used for depiction [36]. Retrieving the features is regarded as the initial phase for image categorization [18]. Here, feature extraction stands for securing the essential data which are required for categorization [19]. Additionally, computer security is also regarded as a significant factor in FR. Because the current system has performed well under relatively controlled

conditions, but it failed to occur when there is a problem with the facial images [20,21]. For example, while presenting a particular face, which may vary in terms of different factors like noise- and blur-induced image damage, make-up, lighting, occlusion, position and posture. Even though the researchers have implemented various techniques and solutions to overcome the issues of this changing condition of the environment, this condition is regarded as a major difficulty of FR [37].

In recent times, various feature extraction process has been designed for a biometric scheme for FR recognition, which are Local Binary Patterns (LBP), Independent Component Analysis (ICA), the histogram method, and Principal Component Analysis (PCA) [22]. In addition to that, CNN techniques have the ability to show the important benefits over the FR model. Along with enhancing DL techniques, the FR framework has accomplished remarkable results [23]. The CNN techniques are usually known as the DNN in terms of computer vision applications that have proved the important benefits of automated visual feature retrieving. Restricted Boltzmann Machine (RBM) techniques have been defined as the generative stochastic unsupervised artificial neural framework, which can potentially learn the probability distribution over its set of inputs [24]. Consequently, many researchers have illustrated by utilizing the deep learning approaches for FR, that are Deep convolutional neural networks (DCNN), Deep Belief Neural Networks (DBN), to robustly identify the human face as well as facial expressions, solve occlusions and illumination variations problems [25]. Hence, the newly suggested FR framework has been developed in this research work.

The major attributions of the FR framework are discussed below:

- To develop the newly proposed Heuristic FR Framework by using the ACLSDN model along with the IHHO algorithm is effectively used for security purposes in fields like banks, airports, and police stations, etc.

- To recommend the new IHHO algorithm derived through the HHO algorithm used for optimal spectral feature selection and parameter optimization in ACLSDN techniques for maximizing the accuracy rate of the given FR model.

- To design the ACLSDN by cascading the scores of the LSTM and DNN model for attaining the classified outcomes from the FR framework and further to enhance the effectiveness of the proposed model IHHO algorithm has been utilized for optimizing the parameters like learning rate, epoch, and hidden neuron count in both the LSTM and DNN model.

- To evaluate various positive and negative metrics to show the superiority of the given FR model in terms of accuracy when assimilated over other models.

The upcoming sections in the FR framework are as follows. Phase 2 gives the literature survey related to the FR model. The proposed architecture and pre-processing done for the face recognition model are in phase 3. Phase 4 shows the dataset model and IHHO for optimal spectral feature selection. Adaptive cascaded deep learning for developing the FR model is in phase 5. Phase 6 represents the results, and the discussion and conclusion are given in Phase 7.

2. Literature Survey
2.1. Related Works

In 2020, Moghaddam *et al.* [1] recommended the double deep learning techniques that involve Recurrent Neural Network (RNN) and LSTM, where the input has been regarded as the VGG-Face descriptions. It has been evaluated by utilizing the VGG-16 CNN framework. The VGG-Face spatial descriptions have retrieved the set of 2D-Sub-Aperture (SA) images rendered through light field images for that various observation angles. Further, the sequence of VGG-Face spatial descriptions has been evaluated using the LSTM model. Then, the overall process was carried out with the standard datasets to address the varied as well as challenging FR tasks. The outcomes have shown that the suggested model has attained greater FR performance when assimilated over others.

In 2021, Chen *et al.* [2] suggested a novel methodology for resolving the quality assessment issues in the classification process. So, particularly, the pair-wise binary quality pseudo-code has been produced without acquiring any additional manual annotations. Further, the detection quality loss has been utilized to decouple the pair-wise network training model. Additionally, a light weighted quality network was trained through the performance for predicting the branch of the FR framework. The investigation has shown that the recommended network has attained greater outcomes.

In 2020, Roy *et al.* [3] proposed a novel method depending on the continual learning shallow network to be helpful for the Heterogeneous Face Recognition (HFR) framework. Further, the proposed model was split into two major regions. In the initial phase, a modality-variant CNN framework utilized the LFrBP feature and then fine-tuned the CNN model. Secondly, it has depended on continual learning to integrate two HFR scenarios by utilizing a single network. Recognition outcomes over various difficult datasets indicate that the proposed model has a higher value than other deep learning-based models.

In 2019, Ni *et al.* [4] designed a significant information framework. It has learned the distance metric by exploring the discriminative information between the interclass neighborhood samples. Here, the distance among the interclass neighborhood samples was as far as possible, and the orientation among the intraclass neighborhood samples was as small as possible. The suggested framework has

learned the hierarchical nonlinear transformations through combining metric learning into the multi-task DCNN. The commonly shared layer propagates the common transformation with the aid of multiple tasks. The other independent layers have learned individual task-special transformations for each task. Investigational outcomes have shown satisfactory performance in terms of accuracy.

In 2021, Khan *et al.* [5] have recommended deep learning techniques, which it has incorporated the simple noise depended on data augmentation for processing FR. The recommended techniques have identified the face in images by utilizing the standard face detector mechanism and then classified it using a trained CNN for tuning the DIFR. While transfer learning, a trained CNN learns the disguise-invariant features through facial images of various subjects to detect the under varying facial disguises. At the end correctly, promising outcomes have been acquired with maximized efficiency rate.

In 2022, Sreekala *et al.* [6] designed novel ensemble-based FR techniques. The designed model was primarily concerned with rapidly and reliably recognizing faces in the input. In addition to that, the model has two pre-processing phases, noise reduction and data augmentation using Bilateral Filtering (BF). Further, by utilizing the ECN model, feature vectors have been extracted. On the other hand, the designed algorithm was utilized for classifying and identifying the faces in the images. Hence, the GWOECN-FR model was evaluated using a standard dataset, and the outcomes were analyzed.

In 2020, Sarhan *et al.* [7] proposed meta-heuristic techniques for classifier framework. Here, the suggested classifier model has been utilized to speed up the feature extraction process. The investigational outcomes have shown that the suggested classifier has provided promising outcomes regarding various performance measures when assimilated over the conventional networking model. In the end, the comparison was empirically utilized to ensure the robustness of the suggested model.

In 2021, Ahmed et al. [8] recommended the Gabor Wavelet transform (GWT) framework. Here, the proposed FR model has been developed for utilizing it for different purposes. Further, the feature extraction from the symmetry face training data was done with the aid of the GWT model, and deep learning techniques were used for FR. The implementations of this proposed model, along with the huge amount of training image samples, have shown the model's effectiveness more than other models.

2.2. Problem Specifications

Recently, appearance-dependent techniques have influenced the FR model due to its simplicity and good performance. Moreover, the huge intra-personal variation such as expression, illumination, and pose are still obstacles because of their changing appearance and self-occlusion. Some of the advantages and disadvantages of the traditional FR model are given in Table 1. CNN [1] techniques are widely used in various applications, specifically real-time applications. It has attained superior performance over other state-of-the-art approaches. But, it failed to face the huge variation in the biometric data characteristics. LightQNet [2] technique is used for enhancing medical treatment.

It can increase the quality of the facial image in the input data. It has low reliability, which degrades the performance of the model. The CNN [3] model does not require human supervision to perform the detection process. It provides outcomes with a high accuracy rate. It needs more time to train the data in the initial stage. MDML-BDI [4] model has the ability to provide both boundary geometry information and discriminative information that aid the FR model. It is distinctively better when compared with other models of recognizing the face. It failed to perform over large-scale FR datasets. CNN [5] model is simple and effective in performing the data augmentation process to retrieve robust features.

The generalization ability of this model is very effective. Insufficient illumination and night-time operation are needed to be explored. GWOECN-FR [6] technique is used for parameter tuning and minimizing the noise in the given image. A hybrid deep learning model, along with a hyperparameter optimizer, is not detailed in this model. CADLVQ [7] technique can detect multi-view face imaging processes with higher accuracy. It requires less storage and computational cost. It faced a challenge while spoofing attacks, which happened by fake subjects. The Gabor wavelet transform [8] model has effectively enhanced the performance of the FR system. It has used the symmetry procedure in feature space and image space. It requires high computational costs.

3. Proposed Architecture and Pre-processing Done for Face Recognition Model

3.1. Face Recognition Framework

FR framework is considered the smallest portion of the facial image processing application, and its importance in the research field is increasing day by day. FR systems are commonly employed as well as preferred for people and security cameras in metropolitan life. This framework is highly utilized to reduce the crime rate, verification, and security processes.

Table 1. Advantages and disadvantages of the traditional FR model

Author [Citation]	Methodology	Features	Challenges
Moghaddam *et al.* [1]	CNN	• These techniques are widely used in various applications, specifically in real-time applications. • It has attained superior performance over other state-of-the-art approaches.	• But, it failed to face the huge variation in the biometric data characteristics.
Chen *et al.* [2]	LightQNet	• This technique is used for enhancing medical treatment. • It has the ability to increase the quality of the facial image in the input data.	• It has low reliability, which degrades the performance of the model.
Roy *et al.* [3]	CNN	• This model does not acquire any human supervision for performing the detection process. • It provides outcomes with a high accuracy rate.	• It needs more time to train the data in the initial stage.
Ni *et al.* [4]	MDML-BDI	• This model has the ability to provide both boundary geometry information and discriminative information that aid the FR model. • It is distinctively better when compared with other models of recognizing the face.	• It failed to perform over large-scale FR datasets.
Khan *et al.* [5]	CNN	• This model is simple as well as effective in performing the data augmentation process to retrieve robust features. • The generalization ability of this model is very effective.	• Insufficient illumination and night-time operation are needed to be explored.
Sreekala *et al.* [6]	GWOECN-FR	• This technique is used for parameter tuning and minimizing the noise in the given image.	• A hybrid deep learning model, along with a hyperparameter optimizer, is not detailed in this model.
Sarhan *et al.* [7]	CADLVQ	• This technique has the ability to detect multi-view face imaging processes with higher accuracy. • It requires less storage and computational cost.	• It faced a challenge while spoofing attacks, which happened by fake subjects.
Ahmed *et al.* [8]	Gabor wavelet transform	• This model has effectively enhanced the performance of the FR system. • It has used the symmetry procedure in feature space and image space.	• It requires high computational costs.

It has been defined as the eminent biometric depended techniques that are used for identity authentication. Moreover, the FR system's major difficulty is regarded as failing to address uncontrolled facial changes. It is also considered the subdivision issue over visual pattern recognition. Through the application layout of the FR model, it is widely utilized in attendance access control, network information security, government management, and so on. In the case of security, both the trace of suspects and early warning of suspicious situations are completed with the assistance of FR. FR system is considered complex image processing issues in terms of real-time applications and the complex effects of imaging conditions on live images, occlusion, and illumination. It is an integration of both FR and detection processes in image analysis. Here, the recognition algorithm has been utilized to categorize the given images and the well-known structure property generally utilized in computer vision applications. Consequently, the detection application is highly used to detect the orientation of the face in the given image. Usually, the recognition application utilizes the standard images as well as the detection algorithm to identify the faces and then retrieve the face images that include nose, mouth, eyes, and eyebrows. Most of the conventional FR system is highly impacted by imaging conditions, facial expression, presence or absence of structural components, pose, and so on. It is difficult for most traditional methods to handle such problems in the FR framework. So, there is a requirement for a well-structured FR application system. Therefore, this research has implemented the robust FR framework for detecting the face, and the architectural process is depicted in Fig. 1.
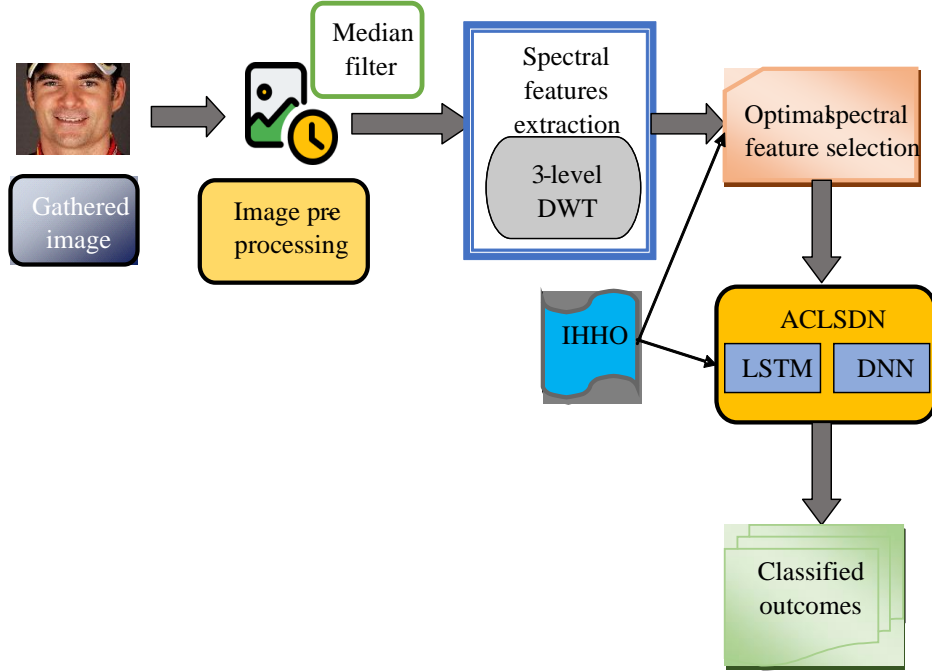
Fig. 1 Architectural model for FR framework using adaptive cascaded deep learning

The newly proposed FR framework has been designed by undergoing the upcoming phases. In the initial phase, the relevant image data to perform the FR process are gathered from the standard dataset. It is then fed to the median filtering process in order to obtain the pre-processed images. Then, it is subjected to the three-level DWT techniques to attain the spectral features. Then, these features are optimally selected with the aid of the newly derived IHHO algorithm.

Further, it is fed to the ACLSDN framework, where the parameters in the LSTM and DNN have been optimized by utilizing the same IHHO algorithm. In the end, the averaging of the score achieved from both the LSTM and DNN models is taken for providing classified outcomes. Thus, the effectiveness of the suggested FR framework has attained maximized accuracy rate.

3.2. Pre-processing of Input Images

In this stage, the image data acquired through the dataset fc_e has been given to the pre-processing, where the median filtering techniques are used to provide the pre-processed images. Thus, this process has been regarded as the non-linear filtering process utilized for neglecting the unwanted noise from the images. In addition to that, it also suppressed the error and maximised the image's quality. The median filtering process is defined as the filtering processes that are effectively used in the image processing field to maintain the edges during noise removal. It has worked based on window operating techniques by randomly choosing the median intensity from the window. In addition, it also takes averaging between the acquired illustrative pixels in an adjacent manner. It has also

carried out the entire process in a pixel-by-pixel procedure and then replaced them by using the median values of the pixel. Hence, this median filtering process has effectively improved image quality.

Here, the aggregated images from the dataset fc_e have been regarded as a group of variables $fc_e = (fc_1, fc_2, \cdots, fc_E)$, and the filtering process is equated in Eq. (1).

$$mefi(fc_e) = \begin{cases} fc_{A+1} = fc_{ak}, & E = 2A + 1 \\ \frac{1}{2}(fc_{A+1} + fc_X) & E = 2A \end{cases} \tag{1}$$

Here, the term $ak = fc_{A+1}$ depicts the median rank. Then, the intensity value in the median filtering process is given in Eq. (2).

$$cd_{ab,cb} = \underset{(ec,gc)\in\varpi}{med}\left(fc_{ab+ec,cb+gc}\right) \tag{2}$$

Here, the term ϖ denotes the window. Finally, the pre-processed image achieved from utilizing the median filtering techniques is denoted as fc_e^{mef}.

4. Dataset Model and Improved Horse Herd Optimization for Optimal Spectral Feature Selection

4.1. Dataset Model

The data needed for performing the FR framework is congregated from the below-mentioned dataset links.

4.1.1. Dataset 1

This dataset is named CFPW; it includes the "frontal-profile view of some celebrities" and involves 10 frontal images through 500 people from 4 profiles. These details are gathered from "http://www.cfpw.io/": "Access Date: 2022-12-08".

4.1.2. Dataset 2

The information regarding this dataset is gathered from "http://vision.ucsd.edu/content/yale-face-database": "Access Date: 2022-12-08" and has been named as Yale dataset. It consists of a total of 5760 images that are attained from 64 various lighting conditions. These images are taken from 10 individuals under nine different poses.

Finally, the image data required for further processing step in the FR framework from the dataset is indicated as fc_e, $e = 1,2, \cdots, EN$ here, the total number of attained images is given EN, and the sample images gathered from the dataset link is depicted in Fig. 2.

4.2. 3-Level DWT-based Spectral Features

In this phase, the pre-processed image attained by using the median filtering techniques fc_e^{mef} has been fed to the 3-level DWT model for attaining the spectral features from the given images. Spectral features of the images have been utilized for the image classification process. It is considered the process of illustrating the number of gray values in the images. It is made by compressing the image data in a certain manner. Here, the classifiers are trained depending on some labelled texture features as a training set to categorize the unlabelled texture features in the images into the pre-defined form of classes. Thus, it resulted in smaller feature space. In the FR model, the 3-level DWT is used for extracting the spectral features.

4.2.1. 3-Level DWT

DWT is regarded as a kind of orthogonal transform, which is used for many facial image-based applications in feature extraction, speech recognition, and so on. It has

maximized frequency and time resolution when assimilated over Discrete Cosine Transform (DCT). The two dependent processing of the DWT is multi-resolution and image compression, which gives a significant way for decomposed images. The DWT model is highly flexible and efficient in decomposing images into various decomposed or sun-band levels known as wavelets. Usually, the DWT decomposes the given images in the wavelet coefficients. It is utilized for retrieving the features from the images. The process is made using the scaling function $\varphi(n)$ and wavelet function $\gamma(n)$. The major intention of this method is to identify detailed variations. Here, the scaling function has been utilized to approximate original images, and it is equated in Eq. (3) and (4).

$$\varphi(n) = \sum_t l(t)\sqrt{2\gamma}\,(2n - t) \qquad (3)$$

$$\varphi(n) = \sum_t m(t)\sqrt{2\gamma}\,(2n - t) \qquad (4)$$

Consequently, the basic wavelet function is computed through the scaling function. The digital filter co-efficient is termed as $m(t)$ and $l(t)$ ss. It is expressed in Eq. (5).

$$m(t) = (-1)^t l(n - t - 1) \qquad (5)$$

Then, the DWT includes various levels in it. In the first level, DWT has split the given image into four sub-band images, in which every sub-bands image includes one of the low-frequency and high-frequency bands that are termed as AA, AF, FA, and FF, where the diagonal high-frequency sub-band is indicated as FF, the vertical high-frequency sub-band is given as FA, the horizontal high-frequency sub-band is termed as AF and the low-frequency sub-band is depicted as AA. The 3-level DWT decomposition AA3 sub-images are significant to minimize the size of the input images and retrieved features for storing in the feature vector. During this process, the spectral features from images are attained by using the 3-level DWT, which is indicated as FS_{gs}^{dwt}, $gs = 1,2, \cdots, Gs$, where the total number attained spectral features from the images are given as Gs.

Description	1	2	3	4	5
Dataset 1					
Dataset 2					

Fig. 2 Sample images attained from two datasets for depicting the FR framework

4.3. Feature Selection by Proposed IHHO
The newly suggested IHHO algorithm has been derived by utilizing the HHO [26] algorithm. The HHO algorithm is significantly used to search the feature space. It also enhances the categorization accuracy, selected number of features, and fitness values. However, it has faced issues when transformed to binary form and failed to address the discrete optimization issues.

In order to tackle these problems in the conventional HHO algorithm, the IHHO algorithm has been developed by using the random number, which is given in Eq. (6).

$$D = \frac{(of_{current} - of_{min}())}{(ofmin_{max})} \quad (6)$$

Here, the minimum fitness value is indicated as of_{min}, the current fitness value is given as $of_{current}$, the maximum fitness value is denoted as of_{max} and the random number among the range [0, 1] is termed as D.

The HOA has been developed by keenly observing the herding mannerism of the horse. It has included six different phases to run the entire process. At iteration, the horses have been moved to correspond to Eq. (7).

$$S_a^{b,ag} = \vec{A}_a^{b,ag} + S_a^{(b-1),ag}, ag = \omega, \xi, \psi, \zeta \quad (7)$$

Here, the velocity vector of ath horse is indicated as $\vec{A}_a^{b,ag}$, the term $S_a^{b,ag}$ denotes the new position of the ath horse at b^{th} iteration, and the old position of the ath horse is given as $S_a^{(b-1),ag}$

4.3.1. Grazing
Like other plants depend on an algorithm, the horse also mostly depends on the grass for survival. The social mannerism of grazing is expressed in Eq. (8).

$$Gz_a^{b,ag} = g\vec{z}_a^{b,ag}(l + u)\left[S_a^{(b-1),ag}\right], ag = \omega, \xi, \psi, \zeta \quad (8)$$

$$g\vec{z}_a^{b,ag} = g\vec{z}_a^{(b-1),ag} S\sigma_{gz} \quad (9)$$

Here, the lower and the upper grazing space is indicated as l and u, at each iteration. The term $Gz_a^{b,ag}$ denotes the reduced linearly in accordance with a reduction factor termed as σ_{gz}. The ath horse's grazing motion parameter at the bth iteration and the horse's proclivity to graze are given as $Gz_a^{b,ag}$.

4.3.2. Hierarchy
In this phase, the horses are split into two phases in the population, namely: followers and leaders. The follower horse usually follows up with the leaders. Then, the strongest horse is termed as a coefficient rc, and it is given as in Eq. (10).

$$\vec{R}c_a^{b,ag} = r\vec{c}_a^{b,ag}[S_{bst}^{(b-1)} - S_a^{(b-1)}], ag = \omega, \xi, \psi \quad (10)$$

$$r\vec{c}_a^{b,ag} = r\vec{c}_a^{(b-1),ag} S\sigma_{rc} \quad (11)$$

Here, the term $S_{bst}^{(b-1)}$ denotes the best horse location at iteration $(b-1)$, $\vec{R}c_a^{b,ag}$ depicts the level of the horse's hierarchy and $\vec{R}c_a^{b,ag}$ defines the reduced linearly in accordance with a reduction factor is termed as σ_{rc}

4.3.3. Sociability
This phase illustrates the horse's lifestyle when assimilated over other social animals. Here, they have banded together in order to enhance their survival rate as well as make escaping them from the attacking animals. It is defined as the propagation toward the other horses' average position cb, and it is equated in Eq. (12).

$$\vec{C}b_a^{b,ag} = c\vec{b}_a^{b,ag}\left[\left(\frac{1}{Z}\sum_{c=1}^{Z} S_c^{(b-1)}\right) - S_a^{(b-1)}\right], ag = \xi, \psi \quad (12)$$

$$c\vec{b}_a^{b,ag} = c\vec{b}_a^{(b-1),ag} S\sigma_{cb} \quad (13)$$

Here, the social motion vector of the ath horse at the bth iteration is denoted as $\vec{C}b_a^{b,ag}$, at b^{th} iteration, the horse's interest in the herd is indicated as $c\vec{b}_a^{b,ag}$, and the population size is given as Z.

4.3.4. Imitation
A horse usually imitates and learns mannerisms from other horses. Hence, it can attain both good and bad actions through other horses. It is detailed by utilizing the mathematical expression in Eq. (14).

$$M\vec{\imath}_a^{b,ag} = m\vec{\imath}_a^{b,ag}\left[\left(\frac{1}{d^Z}\sum_{c=1}^{d^Z} \hat{S}_c^{(b-1)}\right) - S_a^{(b-1)}\right], ag = \psi \quad (14)$$

$$m\vec{\imath}_a^{b,ag} = m\vec{\imath}_a^{(b-1),ag} S\sigma_{mi} \quad (15)$$

Here, the reduced factor is represented as σ_{mi}, the number of horses in the current population, which are in the fittest location, indicated as d^Z, and the ath horse's motion vector in the orientation of the average of best horses along with the location $\hat{S}$ is termed as $M\vec{\imath}_a^{b,ag}$.

4.3.5. Defending Mechanism
The defending mechanism in the horse involves the process of determining the suboptimal and inappropriate responses. It has been designed in such a way that in the horse's defence, other horses are in the worst location that is away from optimal ones. It is expressed in Eq. (16).

$$F\vec{n}_a^{b,ag} = -f\vec{n}_a^{b,ag}\left[\left(\frac{1}{d^Z}\sum_{c=1}^{d^Z} \hat{S}_c^{(b-1)}\right) - S_a^{(b-1)}\right], ag = \omega, \xi, \psi \quad (16)$$

$$f\vec{n}_a^{b,ag} = f\vec{n}_a^{(b-1),ag} S\sigma_{fn} \qquad (17)$$

Here, the term coefficient$-f$ is considered a negative sign in order to manage the current horse out of the undesirable position; the number of horses in the current population, which are in the worst location, is indicated asd^Z, a reducing factor is termed asσ_{fn}, thea^{th}horse escape vector from the average of the worst horses along with its position $\hat{S}$ is denoted as$F\vec{n}_a^{b,ag}$.

4.3.6. Roam

In this phase; horses roam to seek new pastures and to meet their neighbours. It is expressed in terms of random variables that are equated in Eq. (18).

$$R\vec{m}_a^{b,ag} = r\vec{m}_a^{b,ag} DS_a^{(b-1)}, ag = \psi, \zeta \qquad (18)$$

$$r\vec{m}_a^{b,ag} = r\vec{m}_a^{(b-1),ag} S\sigma_{rm} \qquad (19)$$

Here, the reduction function is indicated as σ_{rm}, and the a^{th}horse's random velocity vector is depicted as$R\vec{m}_a^{b,ag}$, and the random value between [0-1] is termed as D. The pseudo-code for the IHHO algorithm is given in Algorithm 1.

Algorithm 1: IHHO
Initialize the random parameters in HHO
Sort the population
Determine the fitness level
Compute the value of D
Update the velocity and position of the HHO algorithm using Eq. (7) and (18)
End
Return the best solution

4.4. Proposed IHHO-based Optimal Spectral Feature Selection

In this phase, the spectral features attained by utilizing the 3-level DWT technique FS_{gs}^{dwt}have been optimized with the aid of a newly developed IHHO algorithm to get the optimal features. It is defined as the process of minimizing the falsely chosen features into half and managing the true positive value at the same level. It has the potential to effectively choose the adequate variable for enhancing the accuracy rate. In addition to that, it has reduced the computational cost and made the entire process more interpretable. In this model, the IHHO is used to optimize spectral features in the image. Here a total of 10 features are optimized from the spectral features images to carry out the overall FR framework in an effective manner. During this process, optimally selected features obtained with the aid of the IHHO algorithm are termed as OFS_{ds}'here$ds = 1,2,\cdots,10$, and the optimal spectral feature selection process is given in Fig. 3.
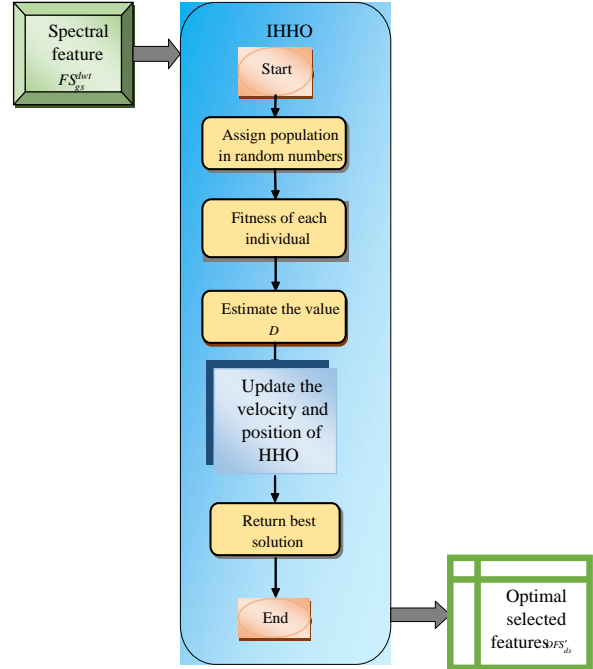

Fig. 3 Diagrammatic depiction of optimal spectral feature selection using the IHHO algorithm

5. Adaptive Cascaded Deep Learning for Developing Model Face Recognition

5.1. Adaptive Cascaded Deep Leaning: ACLSDN

Cascading process in the neural networking model is defined as the process of input-to-output layer mapping of diverse techniques. The cascading process is crucially utilized in the FR techniques because it has the potential to accurately determine the nonlinear relationship between the input and output images without losing the linear relationship from both the networking model. In this suggested FR framework, the DNN and LSTM models are regarded. The outcome obtained using the LSTM model is called score 1, and the outcomes obtained through the DNN model are indicated as score 2. Both these scores attained from the two networking models are taken averaging to obtain the single cascaded output. In this model, the classified outcomes are attained from the FR framework. Then, the adaptive scheme process is determined as optimizing parameters in the networking model to attain the maximized accuracy. In DNN, it has permitted the multiple layers to become more effective at the complex learning features as well as to manage the computational tasks in the network in a significant manner.

On the other hand, it requires a huge amount of data to show better results and is expensive too.

Consequently, the LSTM model does not require any kind of fine adjustment to enhance its performance of the model. It has neglected the unwanted information from the network model and overcomes the vanishing gradient issues. However, it faces difficulty with fitting and memory storage issues. To tackle the issues in the traditional LSTM and DNN model, the

ACLSDN framework has been designed to maximize the accuracy rate of the FR model; it is made by using the objective function given in Eq. (20).

$$of = \underset{\{OFS'_{ds},hc_{lstm},hc_{dnn},epo_{lstm},lr_{dnn}\}}{argmin} \left(\frac{1}{Acry}\right) \quad (20)$$

Here, the optimally selected features in the spectral feature among [1-10] are given by OFS'_{ds} the learning rate between [0.01-0.99], and the hidden neuron count among [5-255] in the DNN model is indicated as lr_{dnn} and hc_{dnn}, the epoch value between [50-100] and the hidden neuron count between [5-255] in LSTM model are depicted as epo_{lstm} and hc_{lstm} has been optimized with the utilization of IHHO algorithm to obtain the maximized accuracy range and the objective function of the FR framework is represented as of. Then, the accuracy value included in the objective function is taken as $Acry$ and is equated in Eq. (21).

$$Acry = \frac{(ueve+uene)}{(ueve+uene+fave+fane)} \quad (21)$$

Here, the term s$ueve$, $uene$, $fave$ and $fane$ indicated the "true positive, true negative, false positive, and false negative", and the overall process is represented in Fig.4.
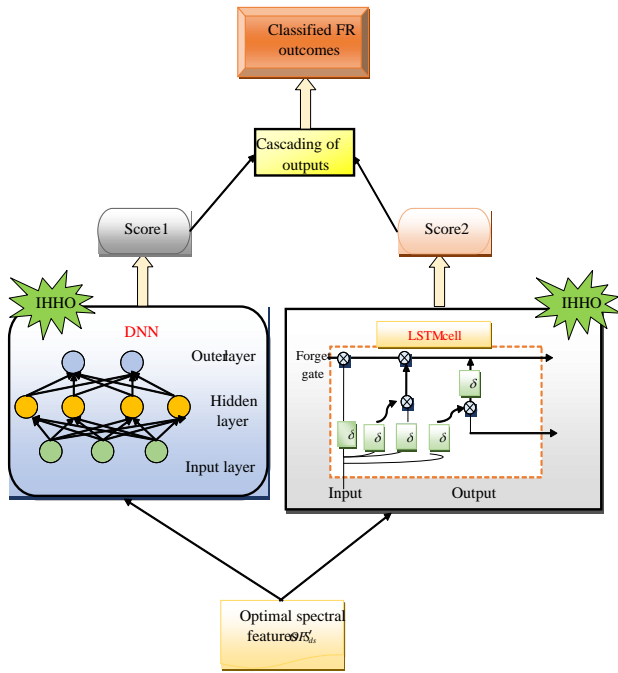
Fig. 4 Diagrammatic representation of ACLSDN process for FR framework

5.2. Describing LSTM and DNN

The optimized spectral features attained with the aid of the IHHO algorithm $\boldsymbol{OFS'_{ds}}$ is fed as the input for both the LSTM and DNN networking model. Using these LSTM and DNN models, the ACLSDN model is introduced to obtain the classified outcomes.

The recurrent neural network (RNN) has been considered a kind of advanced neural networking model. An advanced improvement in the RNN network is known as the LSTM model. It has the ability to memorize the knowledge of the previous output layer when assimilated over the common feed-forward neural network. The individual cells are then joined together to form a huge networking model known as the deep neural network. The cell units have been composed of six major elements and depicted as follows, such as the hidden state, memory state, and the candidate layers are depicted as G, I and $\vec{J}$ accordingly. Then, the output, forget, and input gate is given as kk, ll and mm.

Considering the sequence of vectors $(Y_1, Y_2, \cdots, Y_{cs})$, the hidden layer state G_z of the LSTM at a time z has been computed as in Eq. (22) to (27).

$$fg_z = \pi\left(Y_{z} * M_{fg} + G_{z-1} * N_{fg}\right) \quad (22)$$

$$\vec{J}_z = tanh\left(Y_{z} * M_J + G_{z-1} * N_J\right) \quad (23)$$

$$mm_z = \pi\left(Y_{z} * M_{mm} + G_{z-1} * N_{mm}\right) \quad (24)$$

$$kk_z = \pi\left(Y_{z} * M_{kk} + G_{z-1} * N_{kk}\right) \quad (25)$$

$$J_z = fg_z * J_{z-1} + mm_z * \vec{J}_z \quad (26)$$

$$G_z = kk_z * tanh(J_z) \quad (27)$$

Here, the sigmoid function is given as π, element-wise multiplication is termed as $*$, element-wise addition is given as $+$, current cell memory vectors for the output, forget and input gate is given as kk, ll and mm is indicated as M, N, current cell output is given as J_z, previous cell memory is denoted as J_{z-1}, previous cell output is termed as G_{z-1} and the input vector is depicted as Y_z. During this process, the outcomes obtained by using the LSTM model are indicated as score 1.

The neural networking framework has been defined as the crucial process for recognizing the image pattern. Its networking model is effectively utilized to transform real-time data into numerical vectors. It usually consists of various layers, which are designed through multiple nodes. Depending on the network pattern type, each input image is subjected to the node with some weights. Thus, this acquired weight has been utilized to demonstrate the importance of the input images in providing the final outcomes. Some activation function has carried out the mapping of input to the output. The major intention of this networking model is to approximate some function termed as fn. Here, the classifiers function is indicated as $fn(h)$ has been mapped to the input image OFS'_{ds} to the class denoted as i, where the neural network detects the parameters as ε, resulting in the best approximation function that is expressed as $i = fn(OFS'_{ds}, \varepsilon)$. On training, the desired output of each layer is hidden or invisible, and then it is called a hidden layer.

Then, the width of the DNN was demonstrated through the dimensionality of the hidden layer. Thus, the values of hidden layers are computed by using the activation function. DNN has reduced the cost function among the actual and predicted labels. In recent years, it has been suggested to utilize Relu as the activation function. Then, the single hidden unit activation termed as $hd^{(j)}$ is represented in Eq. (28).

$$hd^{(j)} = v\left(WT^{(j)C} \dots OFS'_{ds}\right) \tag{28}$$

Here, the input images are depicted as OFS'_{ds}, the weighted vector for the jth hidden unit is given as $WT^{(j)}$ and the $tanh$ function is represented as $v()$. During this process, the result obtained by using the DNN model is termed as score 2.

6. Results and Discussion

6.1. Simulation Setup

The proposed FR framework was validated in Python, and the working performance of the FR model was compared with different positive and negative measures. It includes factors such as the maximum number of iterations 25, the number of population 10, and the length of chromosomes 14 were regarded. The algorithm and classifiers such as "Deer Hunting Optimization Algorithm (DHOA) [27], Whale Optimization Algorithm (WOA) [28], Chimp optimization algorithm (CHOA) [29] and Deep Convolutional Neural Networks (DCNN) [30]" were utilized for evaluation.

6.2. Performance Metrics

Various performance measures utilized for validating the FR model are given below:

(a) FPR is in Eq. (29).

$$f = \frac{fave}{fave+uene} \tag{29}$$

(b) FNR is in Eq. (30).

$$fr = \frac{fane}{ueve+uene} \tag{30}$$

(c) Precision is in Eq. (31).

$$pis = \frac{ueve}{ueve+fave} \tag{31}$$

(d) F1 score is in Eq. (32).

$$fs1 = \frac{sn \cdot pis}{pis+sn} \tag{32}$$

(e) Sensitivity is in Eq. (33).

$$sn = \frac{ueve}{ueve+fane} \tag{33}$$

(f) Specificity is in Eq. (34).

$$sc = \frac{uene}{uene+fave} \tag{34}$$

(g) NPV is in Eq. (35).

$$vpn = \frac{fane}{fane+uene} \tag{35}$$

(h) FDR is in Eq. (36).

$$dr = \frac{fave}{fave+ueve} \tag{36}$$

(i) MCC is in Eq. (37).

$$M \frac{ueve \times uene - fave \times fane}{\sqrt{(ueve+fave)(ueve+fane)(uene+fave)(uene+fane)}} \tag{37}$$

6.3. Validating the Performance of the FR Model using Algorithms

Fig. 5 and 6 has depicted the performance of the FR framework over various algorithms for datasets 1 and 2. In Fig. 5 (a), the recommended IHHO-ACLSDN model has 5%, 5%, 4%, and 3% superior to DHOA-ACLSDN, WOA-ACLSDN, CHOA-ACLSDN, and HHO-ACLSDN for accuracy at 85%. Hence the FR model has shown maximized outcomes over other models.

6.4. Validating the Performance of the FR Model using Classifiers

The performance of the FR framework over various classifiers for datasets 1 and 2 are depicted in Fig. 7 and 8. The value of the F1-score on varying the learning percentage at 35 for dataset 1, the recommended IHHO-ACLSDN is 56%, 58%, 53%, and 51% higher than DCNN, LSTM, DNN, and LSTM-DNN model. Therefore, the performance of the FR framework over various classifiers has shown better results.

6.5. Analyzing the Performance of the FR Model using k-fold Over Algorithms

The performance analysis of the FR model using K-fold for various algorithms is given in Fig. 9 and 10. The precision value in Fig.9 (e) at k-fold 3 in the IHHO-ACLSDN model has 51%, 43%, 34%, and 32% higher than DHOA-ACLSDN, WOA-ACLSDN, CHOA-ACLSDN, and HHO-ACLSDN. Thus, the recommended model has shown maximized performance.

6.6. Analyzing the Performance of the FR Model using k-fold Over Classifiers

Fig. 11 and 12 represent the performance analysis of the FR model using K-fold for various classifiers. The recommended IHHO-ACLSDN model is 77%, 78%, 74%, and 63% DCNN, LSTM, DNN, and LSTM-DNN model and shows the greater performance of the model.

6.7. Overall Performance Validation of the FR Model using Algorithms

Tables 2 and 3 depicted the performance of the FR framework over various algorithms for datasets 1 and 2. In Table 2, the recommended IHHO-ACLSDN model has 4%, 4%, 2%, and 1% superior to DHOA-ACLSDN, WOA-ACLSDN, CHOA-ACLSDN, and HHO-ACLSDN for specificity. Hence, the FR model has shown maximized accuracy outcomes over other models.

6.8. Overall Performance Validation of the FR Model using Classifiers

The performance of the FR framework over various classifiers for datasets 1 and 2 are depicted in Tables 4 and 5. The value of the F1-score for dataset 1, the recommended IHHO-ACLSDN, is 58%, 54%, 50%, and 35% higher than DCNN, LSTM, DNN, and LSTM-DNN model. Therefore, the

performance of the FR framework over various classifiers has shown better results.

6.9. Statistical Analysis for Dataset 1

The statistical analysis for datasets 1 and 2 for various algorithms and classifiers is given in Tables 6 and 7. The recommended IHHO-AC attained better values, enhancing the FR framework's performance.
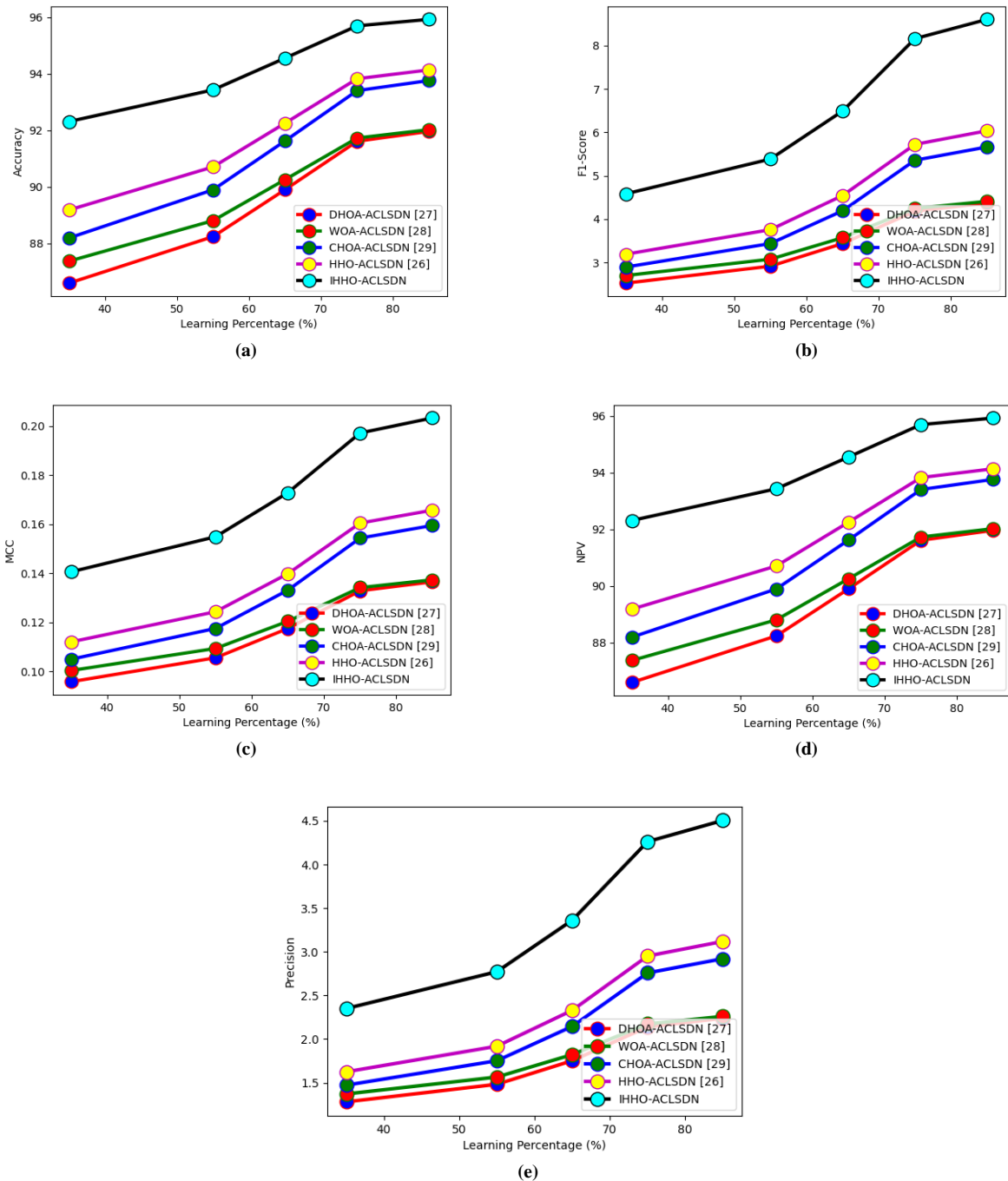
Fig. 5 Validating the performance of FR framework using various algorithms regarding a) Accuracy, b) F1-score, c) MCC, d) NPV, e) Precision for dataset 1
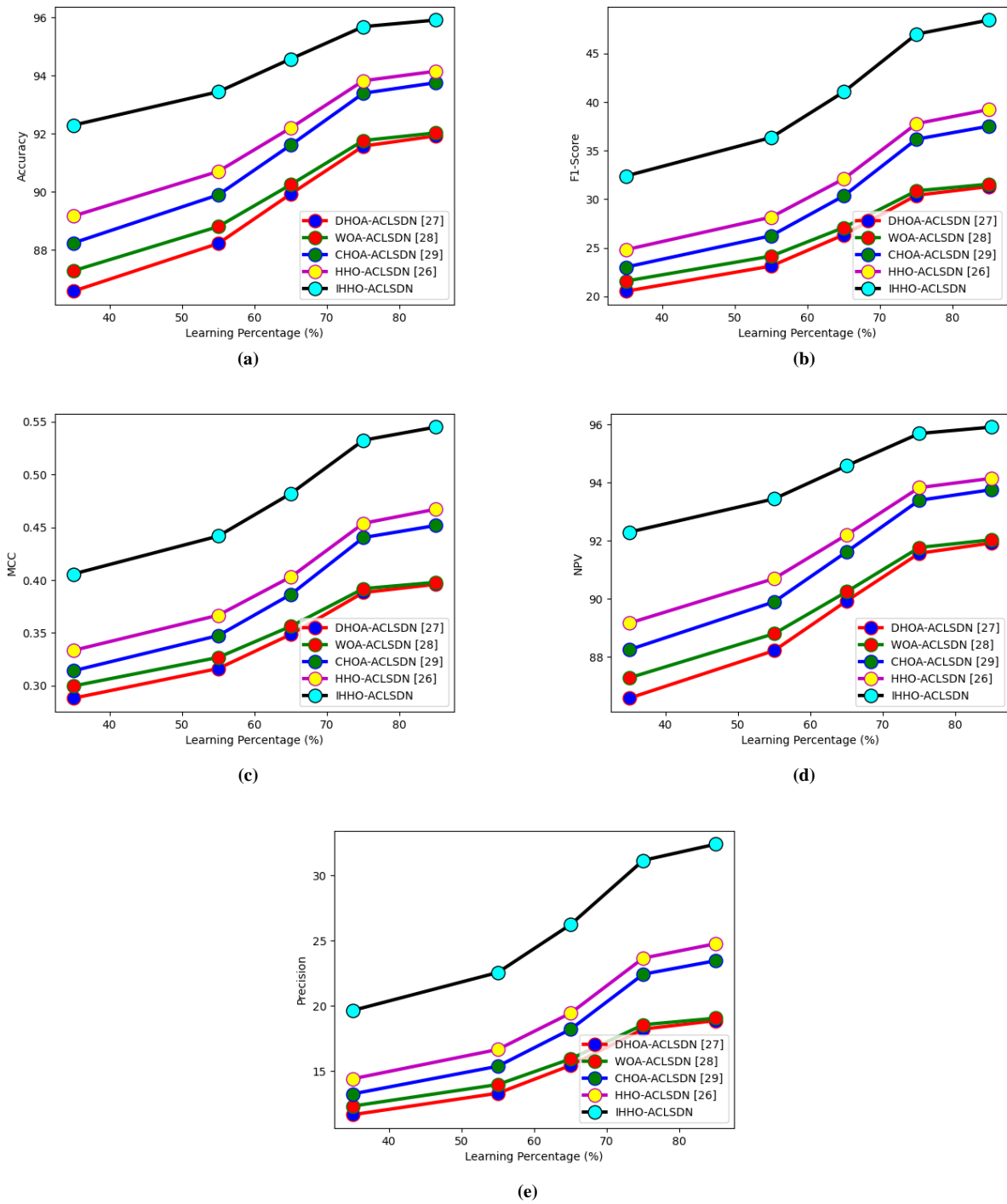
(a)

(b)

(c)

(d)

(e)

Fig. 6 Validating the performance of FR framework using various algorithms regarding a) Accuracy, b) F1-score, c) MCC, d) NPV, e) Precision for dataset 2
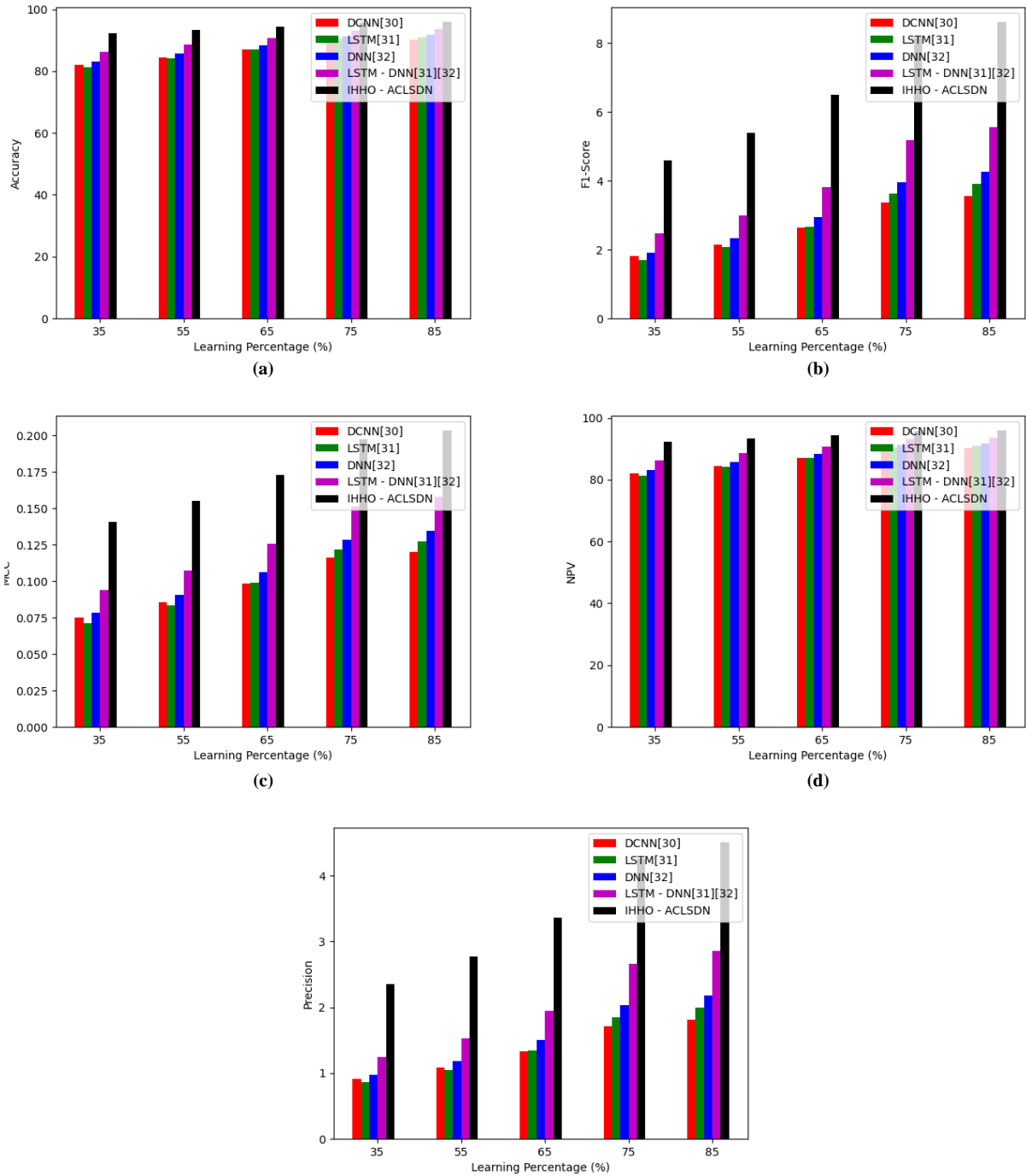
(a)

(b)

(c)

(d)

(e)

Fig. 7 Validating the performance of FR framework using various classifiers regarding a) Accuracy, b) F1-score, c) MCC, d) NPV, e) Precision for dataset 1

(a)

(b)

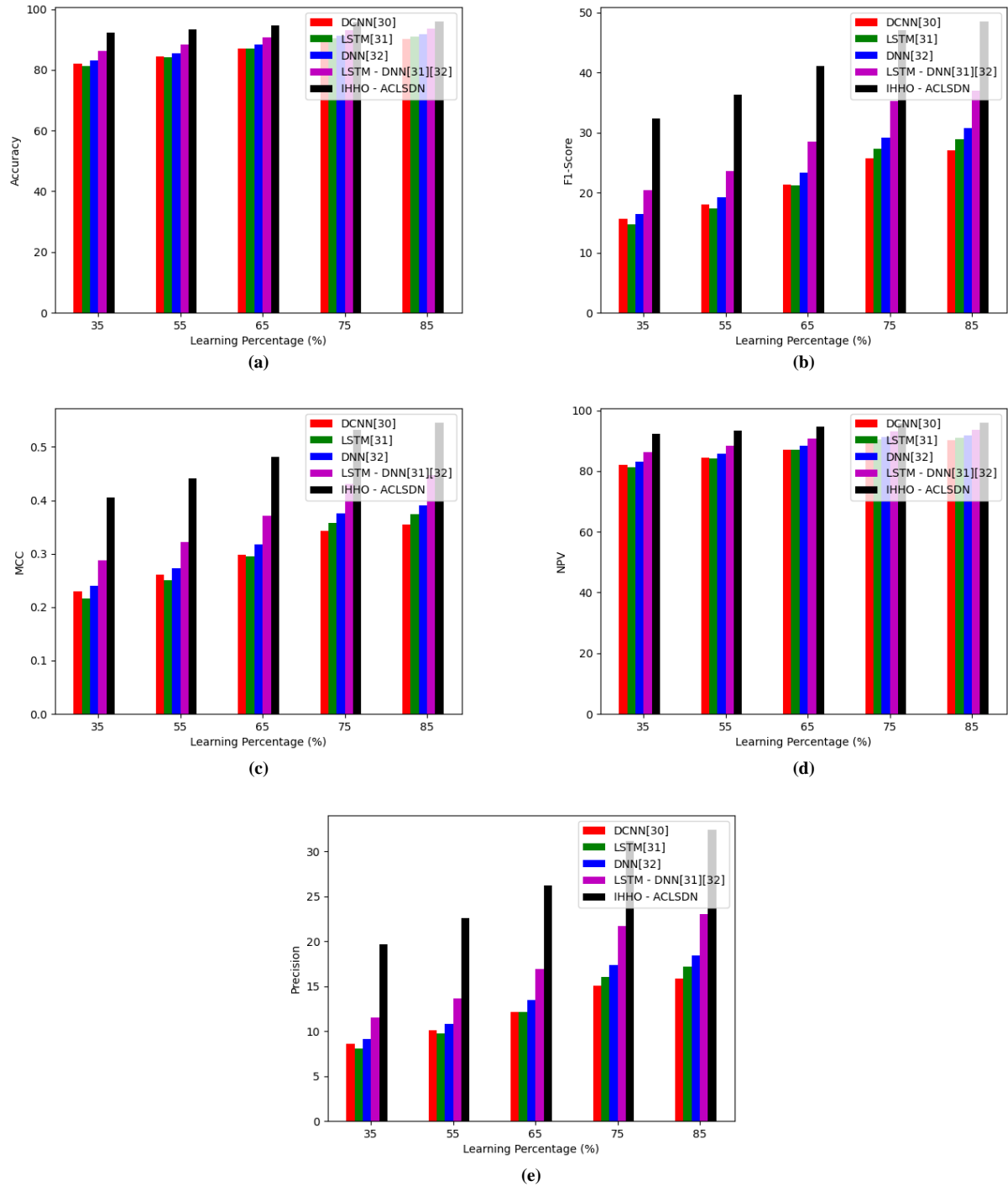**(c)**

(d)

(e)

Fig. 8 Validating the performance of FR framework using various classifiers regarding a) Accuracy, b) F1-score, c) MCC, d) NPV, e) Precision for dataset 2

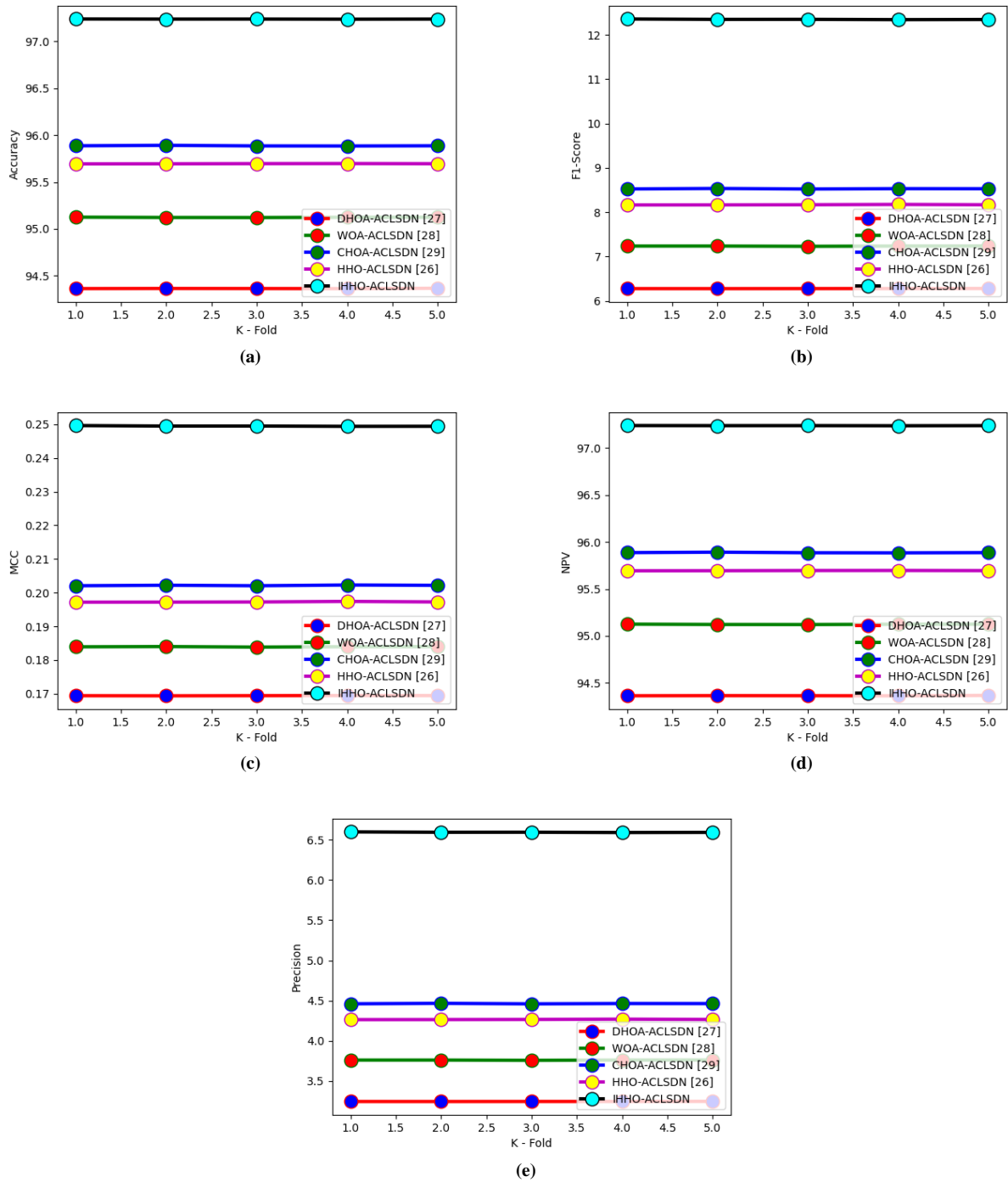**(a)**

(b)

(c)

(d)

(e)

Fig. 9 Analyzing the performance of FR framework using k-fold estimation over various algorithms regarding a) Accuracy, b) F1-score, c) MCC, d) NPV, e) Precision for dataset 1

Fig. 10 Analyzing the performance of FR framework using k-fold estimation over algorithms regarding a) Accuracy, b) F1-score, c) MCC, d) NPV, e) Precision for dataset 2

Fig. 11 Analyzing the performance of FR framework using k-fold over various classifiers regarding a) Accuracy, b) F1-score, c) MCC, d) NPV, e) Precision for dataset 1

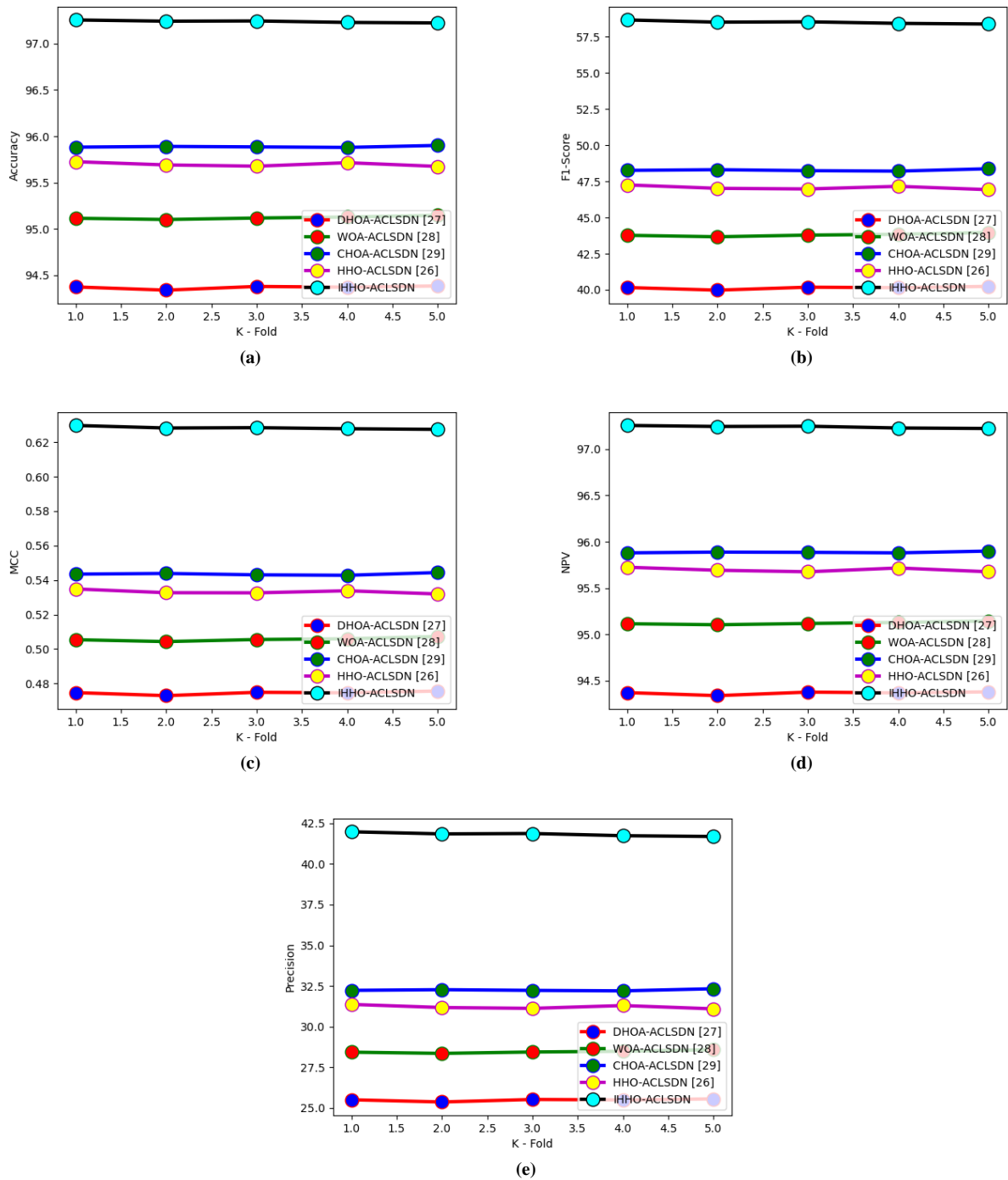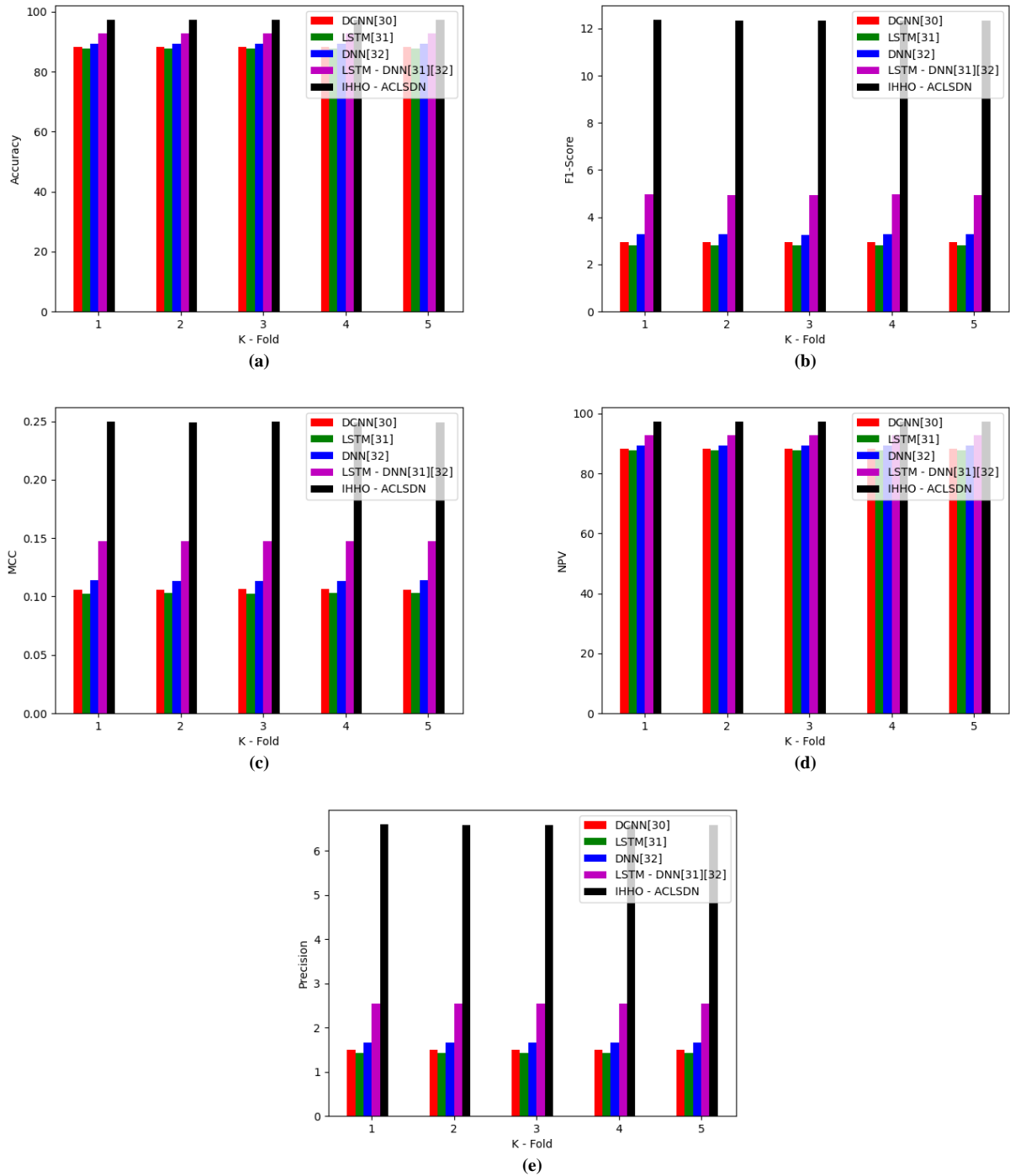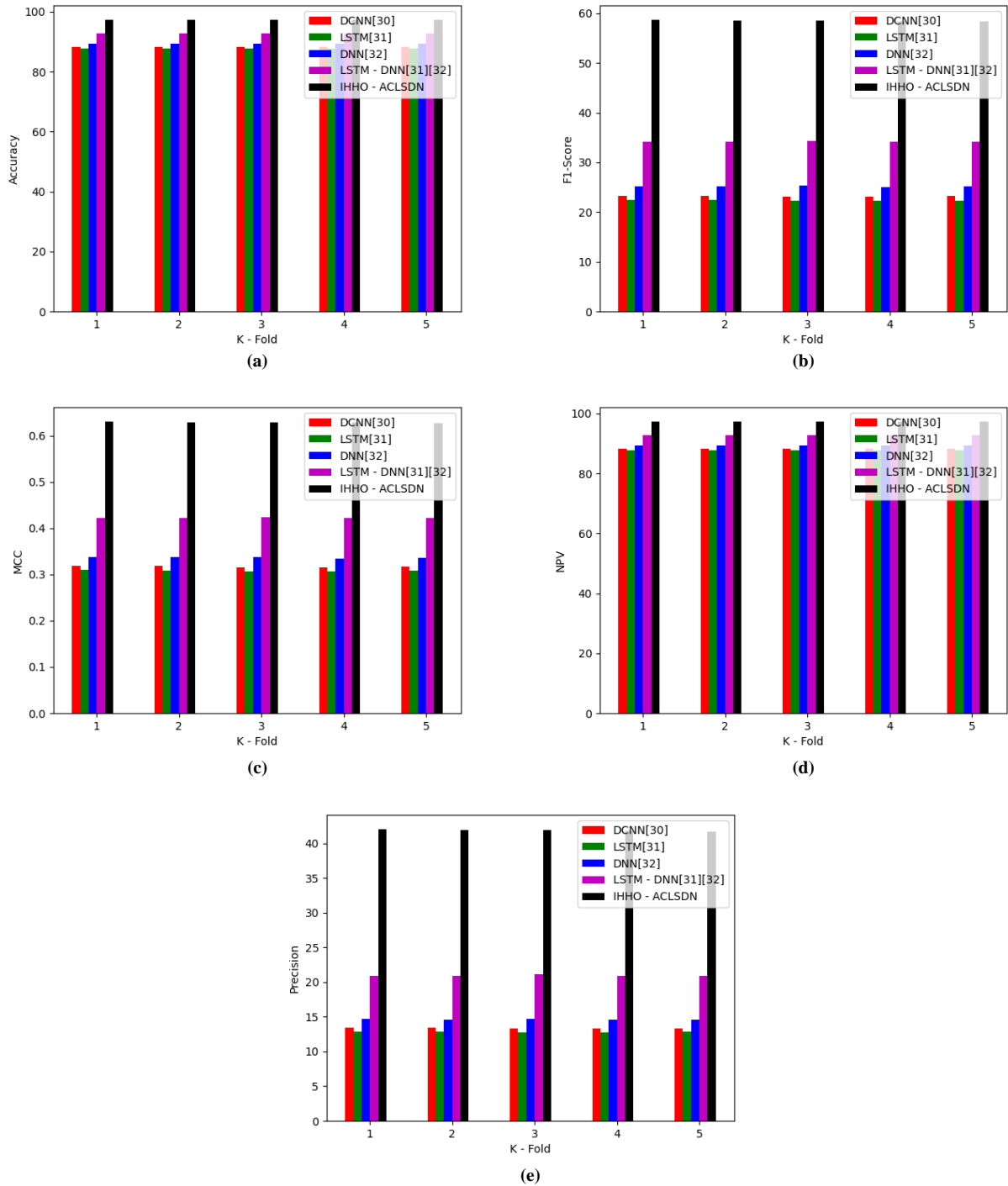**Fig. 12 Analyzing the performance of FR framework using k-fold over classifiers regarding a) Accuracy, b) F1-score, c) MCC, d) NPV, e) Precision for dataset 2**

Table 2. Overall analysis validation for FR model for dataset 1 over algorithms

TERMS	DHOA-ADLSDN [27]	WOA-ADLSDN [28]	CHOA-ADLSDN [29]	HHO-ADLSDN [26]	IHHO-ADLSDN
"Accuracy"	91.96011	92.02086	93.75891	94.13497	95.92443
"Sensitivity"	91.9	92.05714	93.7	94.22857	95.95714
"Specificity"	91.96023	92.02078	93.75903	94.13478	95.92436
"Precision"	2.239419	2.2598	2.920875	3.119148	4.505665
"FPR"	8.039765	7.979216	6.240968	5.865216	4.075637
"FNR"	8.1	7.942857	6.3	5.771429	4.042857
"NPV"	91.96023	92.02078	93.75903	94.13478	95.92436
"FDR"	97.76058	97.7402	97.07913	96.88085	95.49434
"F1-Score"	4.372294	4.411312	5.665152	6.038413	8.60718
"MCC"	0.136498	0.137312	0.159461	0.16569	0.203276

Table 3. Overall analysis validation for FR model for dataset 2 over algorithms

TERMS	DHOA-ADLSDN [27]	WOA-ADLSDN [28]	CHOA-ADLSDN [29]	HHO-ADLSDN [26]	IHHO-ADLSDN
"Accuracy"	91.928	92.032	93.76	94.15467	95.91467
"Sensitivity"	92	91.86667	93.73333	94.4	96
"Specificity"	91.92653	92.03537	93.76054	94.14966	95.91293
"Precision"	18.86792	19.0542	23.46462	24.77257	32.40324
"FPR"	8.073469	7.964626	6.239456	5.85034	4.087075
"FNR"	8	8.133333	6.266667	5.6	4
"NPV"	91.92653	92.03537	93.76054	94.14966	95.91293
"FDR"	81.13208	80.9458	76.53538	75.22743	67.59676
"F1-Score"	31.31382	31.56207	37.53337	39.24612	48.45222
"MCC"	0.396061	0.397942	0.451785	0.467212	0.545019

Table 4. Overall analysis validation for FR model for dataset 1 over classifiers

TERMS	DCNN [30]	LSTM [31]	DNN [33]	LSTM-DNN [32] [33]	IHHO-ADLSDN
"Accuracy"	90.21674	91.02514	91.74249	93.6396	95.92443
"Sensitivity"	90.25714	91.17143	91.75714	93.58571	95.95714
"Specificity"	90.21666	91.02485	91.74246	93.63971	95.92436
"Precision"	1.815256	1.995098	2.178329	2.864251	4.505665
"FPR"	9.783338	8.97515	8.257544	6.360292	4.075637
"FNR"	9.742857	8.828571	8.242857	6.414286	4.042857
"NPV"	90.21666	91.02485	91.74246	93.63971	95.92436
"FDR"	98.18474	98.0049	97.82167	97.13575	95.49434
"F1-Score"	3.558935	3.904749	4.255629	5.558384	8.60718
"MCC"	0.120141	0.127433	0.134308	0.157683	0.203276

Table 5. Overall analysis validation for FR model for dataset 2 over classifiers

TERMS	DCNN [30]	LSTM [31]	DNN [33]	LSTM-DNN [32] [33]	IHHO-ADLSDN
"Accuracy"	90.24	91.03467	91.72533	93.62133	95.91467
"Sensitivity"	90.13333	91.2	91.6	93.73333	96
"Specificity"	90.24218	91.03129	91.72789	93.61905	95.91293
"Precision"	15.8611	17.18593	18.43306	23.0643	32.40324
"FPR"	9.757823	8.968707	8.272109	6.380952	4.087075
"FNR"	9.866667	8.8	8.4	6.266667	4
"NPV"	90.24218	91.03129	91.72789	93.61905	95.91293
"FDR"	84.1389	82.81407	81.56694	76.9357	67.59676
"F1-Score"	26.97526	28.92178	30.69019	37.01948	48.45222
"MCC"	0.354535	0.373769	0.389929	0.447527	0.545019

Table 6. Overall analysis validation for FR model for dataset 1 over classifiers

TERMS	DHOA-ADLSDN [27]	WOA-ADLSDN [28]	CHOA-ADLSDN [29]	HHO-ADLSDN [26]	IHHO-ADLSDN
BEST	1.003293	1.002443	1.003897	1.0056	1.001743
WORST	1.005714	1.013077	1.054209	1.024459	1.010125
MEAN	1.003784	1.00584	1.017985	1.008745	1.002844
MEDIAN	1.003823	1.004062	1.003897	1.00576	1.001743
STD	0.000445	0.004568	0.02259	0.006858	0.002359

Table 7. Overall analysis validation for the model for dataset 2 over classifiers

TERMS	DCNN [30]	LSTM [31]	DNN [33]	LSTM-DNN [32] [33]	IHHO-ADLSDN
BEST	1.002432	1.005617	1.022919	1.005709	1.000516
WORST	1.018495	1.005617	1.105236	1.123942	1.007189
MEAN	1.007436	1.005617	1.035948	1.021781	1.002254
MEDIAN	1.003838	1.005617	1.022919	1.005709	1.000516
STD	0.006922	$2.22 \times^{-16}$	0.017822	0.034202	0.002137

7. Conclusion

This paper has implemented the FR framework with the aid of the ACLSDN model along with the IHHO algorithm for attaining the classified outcomes. Initially, the adequate dataset relevant to the FR process was gathered from the standard dataset. Then, the images were pre-processed with the aid of the median filtering process to attain the pre-processed images. Then, it was given to the three levels-DWT, which were used to attain the spectral features. Then, the features from the spectral features were optimally selected by using the IHHO derived from HHO.

Further, it was subjected to the ACLSDN designed using LSTM and DNN model. It was carried out by averaging the score attained from both the LSTM and DNN models for attaining the classified outcomes in maximized accuracy. Here, the same IHHO algorithm was used for optimizing the parameters in the LSTM and DNN frameworks. The precision value in dataset 2 in IHHO-ACLSDN is 51%, 47%, 43%, and 28%, superior to DCNN, LSTM, DNN, and LSTM-DNN models. Thus, the effectiveness of the designed FR model was validated using various metrics and showed maximized accuracy value.

References

[1] Alireza Sepas-Moghaddam et al., "A Double-Deep Spatio-Angular Learning Framework for Light Field-Based Face Recognition," *IEEE Transactions on Circuits and Systems for Video Technology,* vol. 30, no. 12, pp. 4496-4512, 2020. [CrossRef] [Google Scholar] [Publisher Link]

[2] Kai Chen, Taihe Yi, and Qi Lv, "LightQNet: Lightweight Deep Face Quality Assessment for Risk-Controlled Face Recognition," *IEEE Signal Processing Letters,* vol. 28, pp. 1878-1882, 2021. [CrossRef] [Google Scholar] [Publisher Link]

[3] Hiranmoy Roy, Debotosh Bhattacharjee, and Ondrej Krejcar, "Interpretable Local Frequency Binary Pattern (LFrBP) Based Joint Continual Learning Network for Heterogeneous Face Recognition," *IEEE Transactions on Information Forensics and Security,* vol. 17, pp. 2125-2136, 2022. [CrossRef] [Google Scholar] [Publisher Link]

[4] Tongguang Ni et al., "Multi-Task Deep Metric Learning with Boundary Discriminative Information for Cross-Age Face Verification," *Journal of Grid Computing*, vol. 18, no. 2, pp. 197–210, 2019. [CrossRef] [Google Scholar] [Publisher Link]

[5] Muhammad Junaid Khan et al., "An Automated and Efficient Convolutional Architecture for Disguise-Invariant Face Recognition Using Noise-Based Data Augmentation and Deep Transfer Learning," *The Visual Computer,* vol. 38, pp. 509–523, 2021. [CrossRef] [Google Scholar] [Publisher Link]

[6] Keshetti Sreekala et al., "Capsule Network-Based Deep Transfer Learning Model for Face Recognition," *Wireless Communications and Mobile Computing,* vol. 2022, pp. 12, 2022. [CrossRef] [Google Scholar] [Publisher Link]

[7] Shahenda Sarhan, Aida A. Nasr, and Mahmoud Y. Shams, "Multipose Face Recognition-Based Combined Adaptive Deep Learning Vector Quantization," *Computational Intelligence and Neuroscience,* vol. 2020, pp. 11, 2020. [CrossRef] [Google Scholar] [Publisher Link]

[8] Sulayman Ahmed et al., "Optimum Feature Selection with Particle Swarm Optimization to Face Recognition System Using Gabor Wavelet Transform and Deep Learning," *BioMed Research International,* vol. 2021, pp. 13, 2021. [CrossRef] [Google Scholar] [Publisher Link]

[9] Vinita Bhandiwad, "A Review Paper on 2D to 3D Face Recognition Technology," *SSRG International Journal of VLSI & Signal Processing,* vol. 2, no. 2, pp. 10-13, 2015. [CrossRef] [Publisher Link]

[10] Stan Z. Li et al., "Illumination Invariant Face Recognition Using Near-Infrared Images," *IEEE Transactions on Pattern Analysis and Machine Intelligence*, vol. 29, no. 4, pp. 627-639, 2007. [CrossRef] [Google Scholar] [Publisher Link]

[11] Ran He et al., "Wasserstein CNN: Learning Invariant Features for NIR-VIS Face Recognition," *IEEE Transactions on Pattern Analysis and Machine Intelligence*, vol. 41, no. 7, pp. 1761-1773, 2019. [CrossRef] [Google Scholar] [Publisher Link]

[12] Yueqi Duan et al., "Context-Aware Local Binary Feature Learning for Face Recognition," *IEEE Transactions on Pattern Analysis and Machine Intelligence*, vol. 40, no. 5, pp. 1139-1153, 2018. [CrossRef] [Google Scholar] [Publisher Link]

[13] Guodong Guo, and C. R. Dyer, "Learning from Examples in the Small Sample Case: Face Expression Recognition," *IEEE Transactions on Systems, Man, and Cybernetics, Part B (Cybernetics),* vol. 35, no. 3, pp. 477-488, 2005. [CrossRef] [Google Scholar] [Publisher Link]

[14] Opeyemi Oyelesi, and Akingbade Kayode Francis, "Face Recognition for Access Control using PCA Algorithm," *SSRG International Journal of VLSI & Signal Processing*, vol. 4, no. 2, pp. 22-27, 2017. [CrossRef] [Publisher Link]

[15] Jian Zhao et al., "3D-Aided Dual-Agent GANs for Unconstrained Face Recognition," *IEEE Transactions on Pattern Analysis and Machine Intelligence*, vol. 41, no. 10, pp. 2380-2394, 2019. [CrossRef] [Google Scholar] [Publisher Link]

[16] Jie Pan, Xue-Song Wang, and Yu-Hu Cheng, "Single-Sample Face Recognition Based on LPP Feature Transfer," *IEEE Access*, vol. 4, pp. 2873-2884, 2016. [CrossRef] [Google Scholar] [Publisher Link]

[17] Linkai Li et al., "Integrated Access Control System of Face Recognition and Non-Contact Temperature Measurement Based on Arduino," *International Journal of Computer and Organization Trends,* vol. 12, no. 2, pp. 1-5, 2022. [CrossRef] [Publisher Link]

[18] Yong Xu et al., "Data Uncertainty in Face Recognition," *IEEE Transactions on Cybernetics*, vol. 44, no. 10, pp. 1950-1961, Oct. 2014. [CrossRef] [Google Scholar] [Publisher Link]

[19] Luo Jiang, Juyong Zhang, and Bailin Deng, "Robust RGB-D Face Recognition Using Attribute-Aware Loss," *IEEE Transactions on Pattern Analysis and Machine Intelligence*, vol. 42, no. 10, pp. 2552-2566, 2020. [CrossRef] [Google Scholar] [Publisher Link]

[20] Alireza Sepas-Moghaddam et al., "CapsField: Light Field-Based Face and Expression Recognition in the Wild Using Capsule Routing," *IEEE Transactions on Image Processing,* vol. 30, pp. 2627-2642, 2021. [CrossRef] [Google Scholar] [Publisher Link]

[21] Pooja G Nair, and Sneha R, "A Review: Facial Recognition Using Machine Learning," *International Journal of Recent Engineering Science*, vol. 7, no. 3, pp. 85-89, 2020. [CrossRef] [Publisher Link]

[22] Jiwen Lu, Gang Wang, and Jie Zhou, "Simultaneous Feature and Dictionary Learning for Image Set Based Face Recognition," *IEEE Transactions on Image Processing*, vol. 26, no. 8, pp. 4042-4054, 2017. [CrossRef] [Google Scholar] [Publisher Link]

[23] Seyedehsamaneh Shojaeilangari et al., "Robust Representation and Recognition of Facial Emotions Using Extreme Sparse Learning," *IEEE Transactions on Image Processing,* vol. 24, no. 7, pp. 2140-2152, 2015. [CrossRef] [Google Scholar] [Publisher Link]

[24] Shen Yuong Wong et al., "Realization of a Hybrid Locally Connected Extreme Learning Machine with DeepID for Face Verification," *IEEE Access*, vol. 7, pp. 70447-70460, 2019. [CrossRef] [Google Scholar] [Publisher Link]

[25] J. Lu et al., "Ensemble-Based Discriminant Learning with Boosting for Face Recognition," *IEEE Transactions on Neural Networks,* vol. 17, no. 1, pp. 166-178, 2006. [CrossRef] [Google Scholar] [Publisher Link]

[26] Dina A. Elmanakhly et al., "BinHOA: Efficient Binary Horse Herd Optimization Method for Feature Selection: Analysis and Validations," *IEEE Access*, vol. 10, pp. 26795-26816, 2022. [CrossRef] [Google Scholar] [Publisher Link]

[27] G Brammya et al., "Deer Hunting Optimization Algorithm: A New Nature-Inspired Meta-heuristic Paradigm," *The Computer Journal,* 2017. [CrossRef] [Google Scholar] [Publisher Link]

[28] Seyedali Mirjalili, and Andrew Lewis, "The Whale Optimization Algorithm," *Advances in Engineering Software,* vol. 95, pp. 51–67, 2016. [CrossRef] [Google Scholar] [Publisher Link]

[29] M. Khishe, and M.R. Mosavi, "Chimp Optimization Algorithm," *Expert Systems with Applications,* vol. 149, pp. 113338, 2020. [CrossRef] [Publisher Link]

[30] Waseem Rawat, and Zenghui Wang, "Deep Convolutional Neural Networks for Image Classification: A Comprehensive Review," *Neural Computation,* vol. 29, no. 9, pp. 2352–2449, 2017. [CrossRef] [Google Scholar] [Publisher Link]

[31] Dr. Priya Guptaa et al., "Deep Neural Network for Human Face Recognition," *International Journal of Engineering and Manufacturing,* vol. 8, no. 1, pp. 63-71, 2018. [CrossRef] [Google Scholar] [Publisher Link]

[32] Bui Thanh Hung, and Le Minh Tien, "Facial Expression Recognition with CNN-LSTM," *Research in Intelligent and Computing in Engineering,* pp. 549-560, 2021. [CrossRef] [Google Scholar] [Publisher Link]

[33] Prasanna Rajendra et al., "Smart Surveillance Using OpenCV, Motion Analysis and Facial Landmark," *SSRG International Journal of VLSI & Signal Processing,* vol. 7, no. 1, pp. 11-14, 2020. [CrossRef] [Publisher Link]

[34] Jiwen Lu et al., "Learning Compact Binary Face Descriptor for Face Recognition," *IEEE Transactions on Pattern Analysis and Machine Intelligence*, vol. 37, no. 10, pp. 2041-2056, 2015. [CrossRef] [Google Scholar] [Publisher Link]

[35] D. Masip, À. Lapedriza and J. Vitria, "Boosted Online Learning for Face Recognition," *IEEE Transactions on Systems, Man, and Cybernetics, Part B (Cybernetics)*, vol. 39, no. 2, pp. 530-538, 2009. [CrossRef] [Google Scholar] [Publisher Link]

[36] Jiwen Lu, Venice Erin Liong, and Jie Zhou, "Simultaneous Local Binary Feature Learning and Encoding for Homogeneous and Heterogeneous Face Recognition," *IEEE Transactions on Pattern Analysis and Machine Intelligence,* vol. 40, no. 8, pp. 1979-1993, 2018. [CrossRef] [Google Scholar] [Publisher Link]

[37] M. Pang et al., "Iterative Dynamic Generic Learning for Face Recognition from a Contaminated Single-Sample Per Person," *IEEE Transactions on Neural Networks and Learning Systems,* vol. 32, no. 4, pp. 1560-1574, 2021. [CrossRef] [Google Scholar] [Publisher Link]